



PCCP

**Transport of charge carriers and optoelectronic applications
of highly ordered metal phthalocyanine heterojunction thin
films**

Journal:	<i>Physical Chemistry Chemical Physics</i>
Manuscript ID	CP-PER-02-2021-000889.R1
Article Type:	Perspective
Date Submitted by the Author:	26-Mar-2021
Complete List of Authors:	Qian, Chuan; Hunan Normal University College of Physics and Information Science, Sun, Jia; Institute of Super-microstructure and Ultrafast Process in Advanced Materials (ISUPAM), School of Physics and Electronics, Central South University Gao, Yongli; University of Rochester,

SCHOLARONE™
Manuscripts

PCCP

PERSPECTIVE

Transport of charge carriers and optoelectronic applications of highly ordered metal phthalocyanine heterojunction thin films

Chuan Qian,^a Jia Sun^b and Yongli Gao^{*c}Received 00th January 20xx,
Accepted 00th January 20xx

DOI: 10.1039/x0xx00000x

Organic semiconductor thin films based on polycrystalline small molecules have many attractive properties that have already led to applications in optoelectronic devices, which can be produced by less expensive and stringent processes. Conduction of electric charges is typically done in polycrystalline organic thin films. Unavoidably, the crystalline domain size, orientation, domain boundaries and energy level of interface affect the transport of the charge carriers in organic thin films. In this comprehensive perspective, we focus on the highly ordered organic heterojunction thin films fabricated by weak epitaxy growth. Transport of charge carriers in these highly ordered organic heterojunction thin films was systematically studied with various characterization techniques. Recent advances are presented in high performance optoelectronic applications based on the highly ordered organic heterojunction thin films, including organic photodetectors, photovoltaic cells, photomemory and artificial optoelectronic synapses.

1 Introduction

Organic semiconductors have many attractive properties that have already led to applications in electronic and optoelectronic devices.^{1–5} The performance of these organic devices can now rival to the level of amorphous silicon devices, and be produced by less expensive and stringent processes. In addition, the tunable electronic and spectral properties by materials design and selection have attracted considerable interest from the scientific and technological community.^{6,7} Unlike inorganic semiconductors with delocalized energy bands, the organic semiconductors are bonded relatively weakly and form a network of molecules. In organic semiconductor thin films, the discretely overlapping molecules and the energy levels composed of molecular orbitals interact primarily through Van der Waals forces. Compared to the inorganic semiconductors, this inherent property involves localized electrons and decreases the conductivity of organic semiconductors. Besides, when the organic layer deposited on the inorganic substrate, the molecule-substrate interaction and molecule-molecule interaction both affect the arrangement of molecules.

Although conduction of electric charges is often done in polycrystalline materials, the excellent carrier mobility exhibited

in some organic small molecule materials is impressive.^{8,9} Unavoidably, organic semiconductors deposited on an amorphous substrate such as silicon dioxide result in a disordered polycrystalline thin film. In most of organic devices, the crystalline domain size, orientation, domain boundaries (DBs) and energy level of interface affect the transport of the charge carriers. In a disorder organic film, the high-density DBs exist with transport barriers for charge carriers, resulting in spatially abrupt collapse of the π - π stack and inferior device performance.¹⁰ The charge kinetically trapped at the DBs forms as an electrostatic barrier, which has been studied with macroscopic measurements and numerical simulations.^{11,12} Meanwhile, the molecular orientations and the oriented growth of domain greatly affect the height of the barrier at the boundary.^{13,14} As a result, the organic electronic devices with different sizes of domains show a large variation in degradation rate and carrier mobility.^{15–17} In optimizing the performance of organic devices, tremendous progress has been demonstrated to improve the fabrication techniques or design the organic semiconductors.¹⁸ Improving the morphology of organic thin films is an effective approach to fabricate high-performance devices. A highly ordered structure is desired that will provide few charge traps for achieving the charge transport with high efficiency.

In addition, because of the fascinating photo-conducting and photo-detecting characteristics in a wide range of wavelength, the optoelectronic applications based on organic semiconductors have been regarded promising.^{19–23} In particular, artificial optoelectronic synapse has been one of the active research areas in recent years.^{24–28} As a new hardware architecture designed to adapt neuromorphic computing paradigm, artificial synaptic devices break the limitation of data exchange rate between the data-computing and memory units in conventional digital computing systems.^{29,30} For implementation of the biological synaptic dynamics, the artificial synapses based on

^a Synergetic Innovation Center for Quantum Effects and Application, Key Laboratory of Low-dimensional Quantum Structures and Quantum Control of Ministry of Education, College of Physics and Information Science, Hunan Normal University, Changsha, 410081, P.R. China.

^b Hunan Key Laboratory for Super Microstructure and Ultrafast Process, School of Physics and Electronics, Central South University, Changsha, Hunan 410083, P. R. China

^c Department of Physics and Astronomy, University of Rochester, Rochester, NY 14627, USA.

* E-mail: ygao@pas.rochester.edu.

optoelectronic device with sensory functions, integrated signal conversion and information storage have achieved a simulation of visual systems. Processing visual details as sight, a visual system is a unique and important part in biological neural network. In the system the retina is the light-sensitive layer to translates the light signals into electrical pulses, like a photodetector. Therefore, it is meaningful to achieve light signal detection and neuromorphic computing process in the artificial optoelectronic synapse based on highly ordered organic heterojunction thin films.

In this perspective, we review the effect of intro-domains and DBs on charge transport in highly ordered organic heterojunction thin films fabricated by weak epitaxy growth (WEG) method. WEG has been developed to produce high-quality organic semiconductor thin film with controllable morphologies and interface properties. We then describe systematic and in-depth investigations with various characterization techniques on transport of charge carriers in those highly ordered organic heterojunction thin films. Finally, we outline recent advances for optoelectronic applications based on highly ordered organic heterojunction thin films and discuss the existing challenges and functionable applications in the field of artificial intelligence.

2 Highly ordered organic semiconductor thin films

When preparing an organic semiconductor thin film by depositing at a fast rate or spin coating, amorphous morphology is always obtained, as there is not enough time nor energy for creating ordered domains with normal molecule-molecule interactions. The aggregate structure influences the efficiency of charge generation and mobility.^{31,32} Disorder morphology of organic thin films with a lot of boundaries restricts the charge transport. However, with various growth conditions, the arrangement of organic molecules can be different. By just optimizing the parameters of the deposition process such as the temperature of substrate, the morphology of an organic thin film could be improved with better electronic transport properties. The correlation between the substrate heat-treatment conditions and the anisotropic conductivity was reported (Fig. 1).³³ The orientation of crystallites in copper phthalocyanine (CuPc) thin film depended on the temperature of substrate during film deposition. By elevating the substrate temperature, the trap density reduced, and mobility of holes and electrons improved.³⁴

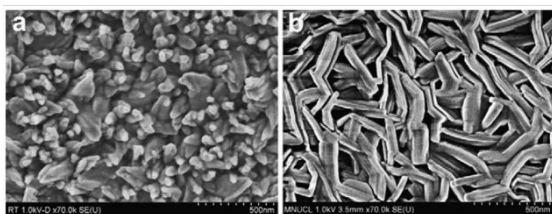


Fig. 1 SEM images of CuPc thin film deposited with a substrate temperature of (a) room temperature and (b) 300 °C.³³ Reproduced with permission from ref. 33. Copyright 2010 Elsevier B.V.

CuPc is considered one of the most common pigments and a well-known *p*-type organic semiconductor with planar phthalocyanine compounds. Because of the large π -conjugated system and unique electronic characteristics, the family of phthalocyanines, especially CuPc, has been widely studied as one of good candidates for organic electronics.^{18,34} Most of metal phthalocyanines (MPcs) are relatively inexpensive to synthesize in large quantities and show a similar structure with a changed central atom. By optimizing the morphology or engineering the interface, the carrier mobility of CuPc devices has been improved.^{35–38} Due to its advantageous attributes such as good stability and strong light absorption, CuPc is also a popular organic photoelectronic material.

As it is known, the continuous structure of single crystals with no boundary produces enhanced conductivity and achieves the best device performance. However, it is hard and not cost effective to fabricate devices based on the single crystals. For the future of organic electronic devices, to prepare an ordered organic semiconductor thin film with a low cost and ease of processing is very important.^{39,40} The conductivity of amorphous structure is limited by the short range order. Highly ordered structure with crystalline or para-crystalline phases will improve the conductivity. Furthermore, highly ordered crystalline organic semiconductor thin films are particularly desirable to obtain high-performance organic field effect transistors (OFETs) and optoelectronic devices.^{41–43}

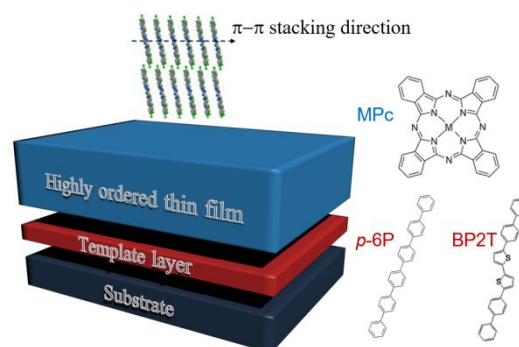


Fig. 2 The schematic of device structure, and molecular structures of MPc, *p*-6P and BP2T.

WEG method was developed specifically to fabricate highly ordered organic semiconductor thin films (Fig. 2).⁴⁴ For the WEG technique, few layers of rod-like molecules are first thermally deposited on an amorphous or polycrystalline substrate as the template layer. Then, the overlayer is induced to grow epitaxially with high quality morphology, which is helpful for improving the device performance. In general, the organic molecules arrange themselves with a lying-down configuration on the amorphous substrate due to the van der Waals forces and other complicated interactions between molecules and substrates. With substrate heating during WEG, the interaction of organic molecules' π - π stacking is stronger than the interaction between the substrate and molecules. As a result, the molecules stand up on the substrate and the direction of π - π interactions would be parallel to the substrate, which is good for the horizontal charge transport.

In the WEG technique, the template layers always use the organic rod-like molecules: *para*-sexiphenyl (*p*-6P) and 2,5-bis(4-biphenyl) bithiophene (BP2T). MPcs have been widely utilized for the fabrication of highly ordered organic semiconductor thin films induced by the template layer. The molecular structures of MPcs are composed of a nitrogen-linked tetrameric diiminoisoindoline conjugated macrocycle chelating a metal atom. Due to the planarity of MPcs molecules, crystalline or polycrystalline films could be formed.

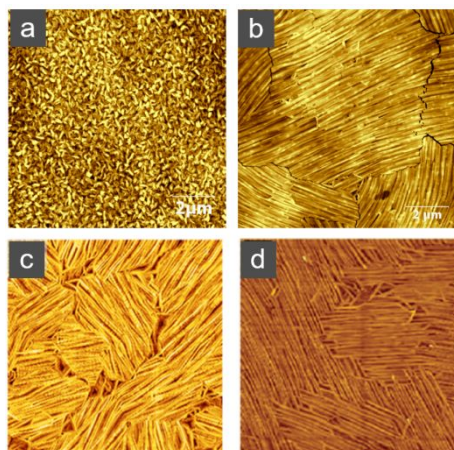


Fig. 3 AFM images of (a) CuPc, (b) CuPc/*p*-6P,⁴⁵ (c) CuPc/BP2T,⁴⁶ and (d) ZnPc/*p*-6P⁴⁷ films. The scan area is 10 μm × 10 μm. Reproduced with permission from ref. 45. Copyright 2016 WILEY-VCH Verlag GmbH & Co. KGaA, Weinheim. Reproduced with permission from ref. 46. Copyright AIP Publishing. Reproduced with permission from ref. 47. Copyright 2007 WILEY-VCH Verlag GmbH & Co. KGaA, Weinheim.

By using this effective technique, highly ordered CuPc/*p*-6P thin films were fabricated. In comparison, the polycrystalline CuPc thin film with many boundaries and small domain size show a disorderly arrangement (Fig. 3a). The size of crystal domain in the highly ordered domain is dependent on the thickness of template layer and the temperature of substrate. Hole transport mainly occurred to molecular planes depending on the π -orbital overlap. Therefore, the work of template layer is important to induce highly ordered MPc thin films for a significant improvement in carrier transport.⁴⁷ Under optimized condition, the size of 100 μm² can be obtained (Fig. 3b).⁴⁵ In the domain, obvious stripe-like order structure was exhibited and the long crystal whiskers with parallel arrangement ensure a better carriers transport. The larger size of domains, the less boundaries to restrict the transport of charge carriers. When the template layer changed to the rodlike molecule of BP2T, the CuPc/BP2T thin film prepared by WEG technique also show the ordered morphology with crystalline domains as shown in Fig. 3c. Up to now, the WEG has been succeeded in preparing various ordered MPc thin films with inserted ultrathin template layer.^{44,46,47}

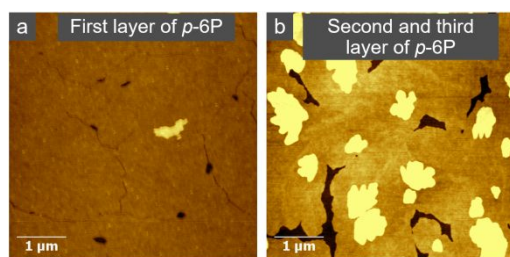


Fig. 4 AFM morphologies of *p*-6P with different coverage grown on SiO₂ substrate.²⁸ Reproduced with permission from ref. 28. Copyright 2019 Elsevier Ltd.

The morphology of MPc thin films grown on *p*-6P layer is very sensitive to the thickness of the template layer.^{48–50} The *p*-6P layer deposited onto the SiO₂ surface shows several discontinuous islands, which is because the *p*-6P film is normally formed through the Stranski–Krastanov growth, i.e., layer-plus-island growth. As the organic molecules start being deposited on the substrate, a critical number of molecules forms the stable nucleus on the substrate. With more molecules absorbed and gathered, islands form, grow, and coalesce each other. The first molecular layer (ML) of *p*-6P gradually covers on the substrate as the second layer begins to form (Fig. 4). When the thickness is above 3 nm, it would show the island growth mode from the second molecular layer. The topographic image of 2.4 ML *p*-6P thin film shows discontinuous islands. The morphology of CuPc strongly depends on the thickness of the *p*-6P layer. The more ordered and preferentially oriented CuPc thin film can grow on the surface of 2.4 ML *p*-6P. The authors suggest that although the template layer increases the number of traps in the thin film, it improves the morphology of the overlayer a lot to increase the carrier mobility.⁴⁸

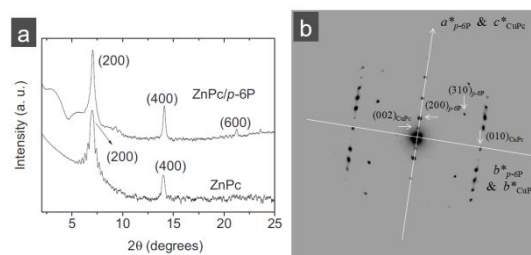


Fig. 5 (a) X-Ray diffraction patterns of ZnPc/*p*-6P and ZnPc thin films⁴⁷. (b) The SAED pattern of CuPc/*p*-6P thin film.⁴⁹ Reproduced with permission from ref. 47. Copyright 2007 WILEY-VCH Verlag GmbH & Co. KGaA, Weinheim. Reproduced with permission from ref. 49. Copyright 2015, American Chemical Society.

By depositing the *p*-6P layer on SiO₂ substrate as a molecular template layer, the MPc layer grows epitaxially on the surface of the *p*-6P layer as a result of lattice match. X-Ray diffraction analysis showed that, compared with zinc phthalocyanine (ZnPc) thin film, the crystallization of ZnPc/*p*-6P thin films was improved and the direction of π - π stacking was parallel to the substrate.⁴⁷ The epitaxial relationship between the MPc layer and template layer was also proved by the selected area electron diffraction (SAED) pattern analysis.^{18,44,51} The SAED pattern of the CuPc/*p*-6P highly ordered thin film directly reveals the crystal lattice correlation between the CuPc and *p*-6P crystals (Fig. 5b).⁴⁹ The confirmed lattice match is (001)*p*-6P//[(100)CuPc], [100]*p*-6P//[001]CuPc, and [010]*p*-6P//[010]CuPc. The molecular crystals of MPc layer are epitaxially oriented relative to the template layer, leading to a highly ordered molecular arrangement. The edge-on orientation and ordered arrangement of MPc molecules are favorable to the horizontal charge transport.

3 Transport of charge carriers

In organic semiconductors, charge transport is affected by the molecules packing arrangements, and π - π stacking is beneficial for improving the transport of charge carriers. The mobility of single-crystal OFET is maximized along the molecular π - π stacking direction.⁴⁹ The anisotropy of charge transport points out that the efficiency of transport is intimately related to the interacting molecules. The charges generally moved from one organic molecule to the next by hopping, therefore, a better spatial overlap between the molecule orbitals in highly ordered thin film is extremely important.⁵² Due to the operation of OFET, significant channel current will be generated when the MPc molecules stand perpendicular to the substrate. For example, the devices based on *p*-type planar phthalocyanine compounds of CuPc and ZnPc have been examined (Fig. 6). On an amorphous substrate, single-MPc-layer devices just show lower channel current. When the π -orbital overlap is unfavourable in conjugated organic semiconductors, charge mobility can be reduced by orders of magnitude.⁵³

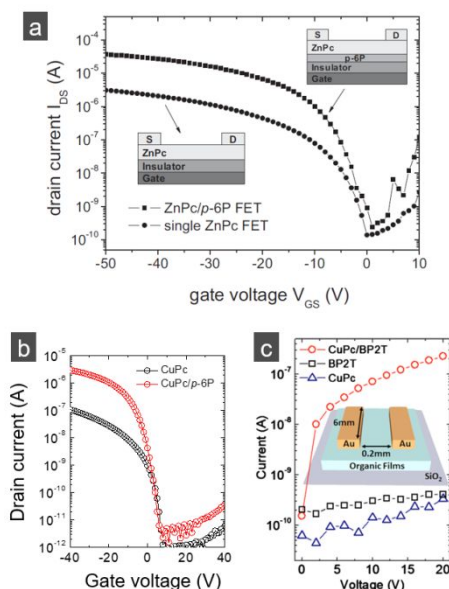


Fig. 6 The comparison of electrical properties between ordered and disordered thin films.^{46,47} Reproduced with permission from ref. 46. Copyright AIP Publishing. Reproduced with permission from ref. 47. Copyright 2007 WILEY-VCH Verlag GmbH & Co. KGaA, Weinheim.

The *p*-6P and BP2T layer as the crystal template improve the crystalline microstructure of the overlying MPc layer and consequently enhance the charge transport property in the channel. The mobility has been greatly improved by the WEG method. Based on the highly ordered ZnPc/*p*-6P thin film, the OFET show a high mobility of $0.32 \text{ cm}^2/\text{Vs}$.⁴⁷ The field-effect mobility has a strong dependence on the size of crystalline domain. The highest value of $0.18 \text{ cm}^2/\text{Vs}$ was obtained with the domain size of $60 \mu\text{m}^2$ in CuPc/*p*-6P thin film, which reached the value in corresponding single-crystalline devices.⁵⁰

Surface: AFM, KPFM, CSAFM and XPS

Horizontally transport of charge carriers

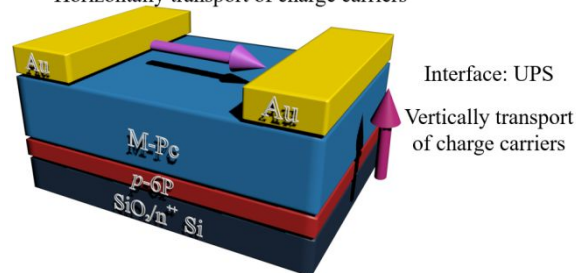


Fig. 7 The horizontally and vertically transport of charge carriers in the highly ordered thin films prepared by WEG method characterized by various characterization instruments.

Compared with the DB-limited transport of charge carriers in a polycrystalline single-MPc thin film, the highly ordered thin film with optimized microstructure shows superior transport properties. However, the MPc layer grown on this *p*-6P surface consists of many separated needle-like crystals. And it is hard to align all crystals in the same direction, showing anisotropic conductivity in each crystalline domain.⁴⁹ Also, the boundaries are appearing in the disconnected area. For better understanding the effect of intro-domains and domain boundaries on charge transport of highly ordered thin films fabricated by WEG, *in-situ* kelvin probe force microscopy (KPFM) was performed. KPFM has proved to be a powerful tool to study the morphological and electronic properties with high spatial resolution. The standard KPFM feedback loop measures the contact potential difference (CPD) between the tip and sample. By detecting the electrostatic-force interaction between the thin film and the tip, the topographical and surface potential (SP) line profiles can be recorded simultaneously.

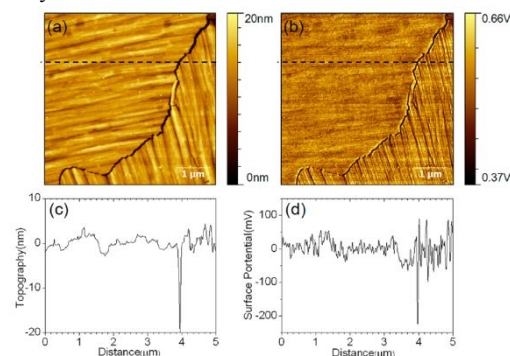


Fig. 8 (a) Topographic image of CuPc/*p*-6P thin film. (b) Corresponding surface potential image. (c) Topographic data for the line section in (a). (d) Surface potential data for the line section in (b).⁴⁹ Reproduced with permission from ref. 49. Copyright 2015, American Chemical Society.

The SP images of CuPc/*p*-6P thin film prepared by WEG method show the detailed electrical properties of the nanostructures (Fig. 8).⁴⁹ In the intra-domain, the SP is at a similar level. And the boundary can be easily observed between two highly oriented domains. The potential well at the boundary is about 0.24 V in depth and 69 nm in width. At the positively charged boundaries, the space-charge region of hole depletion is formed. The back-to-back Schottky barriers restricted the transport of charge carriers. The charge carriers need to go through the potential barrier by thermionic emission. As a result, decrease the number of boundaries leads to the increase of the charge mobility.

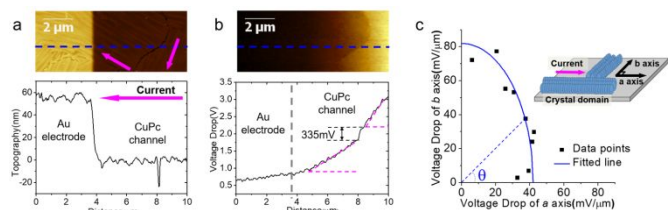


Fig. 9 (a) Topographic image of Au electrodes and CuPc/*p*-6P channel with two different directions of crystalline domains. (b) Corresponding voltage drop image. (c) Correlation between the voltage drop and the angle forming between the current direction along the *a*-axis and the orientation of each domain.⁴⁹ Reproduced with permission from ref. 49. Copyright 2015, American Chemical Society. Reproduced with permission from ref. 50. Copyright 2015 Elsevier.

In particular, *in-situ* KPFM can quantitatively map the voltage drop of nano-objects. The intra-domains and the domain boundaries were systematically investigated by *in-situ* KPFM (Fig. 9).^{49,50} The voltage drop detected by the *in-situ* KPFM in the operating device, which was depended on the domain sizes, orientations, and width of boundaries. At a microscopic level, each domain with different orientation and boundaries with non-uniform trap density in the thin film decide the individual contributions to macroscopic charge transport. The voltage drop increases with the angle θ between the arrangement of domain and the current. The voltage drop is given by the following equation:

$$\Delta V_D = \sum_{i=1}^n \frac{A L_{Di}}{\sqrt{1 + B \cos^2 \theta_i}} \sum_{i=1}^n L_{Di} = L_{ds}$$

where L_{Di} is size of domain and L_{ds} is the length between electrodes. In Fig. 9c, the fitting parameter of magnitude (A) is $82 \text{ mV}/\mu\text{m}^2$ and ellipticity of the voltage drop (B) is 2.81. When the angle equal to zero, the orientation of π - π stacking of the molecules is parallel to the current, the voltage drop is the minimum. For the domain boundaries, more trap states are stay in the boundaries and steep voltage drop (335 mV) occurred here. Because of the existence of traps, the back-to-back Schottky barriers are formed at both sides of boundaries. The voltage drop across the DBs is influenced by the width of boundaries and the angle of neighboring domains. Large angle between the directions of neighboring domains also increased the voltage drop across the DBs. Due to the reduction of boundaries' number and the mismatched orientation degree, highly ordered thin film with large domain size improved the charge transport with high mobility.

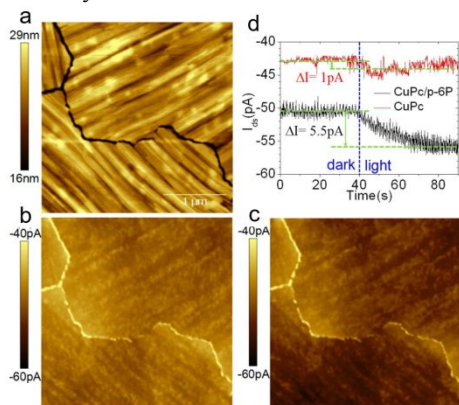


Fig. 10 (a) Topographic images of CuPc/*p*-6P thin film. The corresponding current images (b) under dark and (c) CuPc/*p*-6P thin film under light. (d) The

change of current detected by the tip as function of time under dark (time < 40 s) or under light (time \geq 40 s).⁴⁵ Reproduced with permission from ref. 45. Copyright 2016 WILEY-VCH Verlag GmbH & Co. KGaA, Weinheim.

Besides KPFM, the method of current sensing atomic force microscopy (CSAFM) is also the development in the context of classic AFM to obtain local electronic information. The operation of device based on the organic semiconductor thin films with highly ordered morphologies and molecular orientations under light in nanoscale has been carried out with *in-situ* CSAFM.⁴⁵ The current image shows a remarkable difference between the intra-domains and boundaries (Fig. 10). Because of the single-crystal-like property in intra-domains, more conductive regions with higher current levels evidently exist in domains. Detailed study of the optoelectronic response in nanoscale spatial resolution proved that the photocurrent is predominately produced inside the highly ordered CuPc/*p*-6P heterojunction domains, while the photocurrent produced at the boundaries between domains can be neglected. Therefore, the change of current detected by tip in a CuPc-single-layer thin film is much smaller than that in a CuPc/*p*-6P heterojunction thin film. On the template layer, the highly ordered CuPc film leads to a large improvement in the optoelectronic properties.

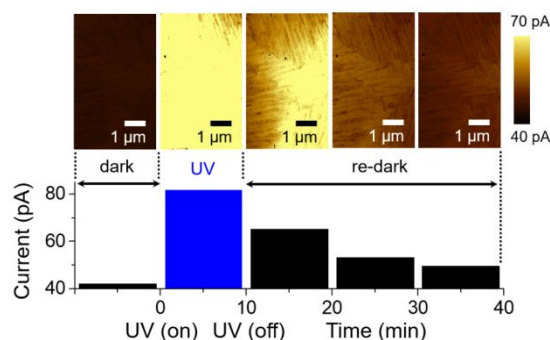


Fig. 11 Time-dependent change in the current mapping of CuPc/*p*-6P thin film after exposure to the 365 nm light pulse, which was detected using CSAFM, and the obtained average current on the surface of each state.²⁸ Reproduced with permission from ref. 28. Copyright 2019 Elsevier Ltd.

In-situ CSAFM has been used to detect the photomemory behavior with a retention photocurrent after a light illumination in highly ordered CuPc/*p*-6P thin film (Fig. 11).²⁸ Under illumination, the average current on the surface increased from 42.3 to 81.9 pA. The region of intra-domain is the most contributing to the photocurrent. After turning off the light, the average current was reduced to 49.6 pA after 30 min, which indicated that approximately 61% of current was retained even after half an hour. In the highly ordered CuPc/*p*-6P film, the holes are transferred from *p*-6P layer to CuPc layer, and the remaining electrons are probably trapped in *p*-6P layer, which cause an asymmetric carrier distribution. Consequently, the holes stored in the CuPc layer for a long time with little recombination. For the CuPc-only device, the current returned to its initial current in a short time, owing to the symmetric distribution of photo-generated electrons and holes. The study shows that *in situ* CSAFM is useful for understanding the factors affecting the generation and transport of charge carriers in nanostructure under illumination.

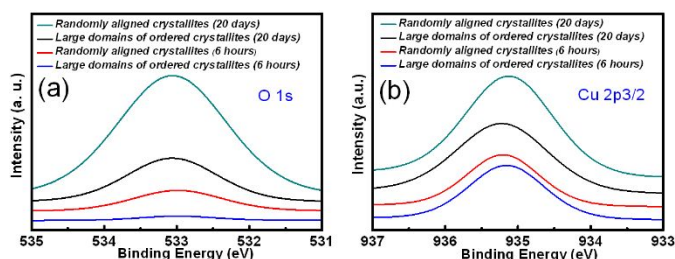


Fig. 12 (a) XPS O 1s spectrum and (b) Cu 2p_{3/2} spectrum of CuPc thin film after 6 hours and 20 days in ambient.⁵⁰ Reproduced with permission from ref. 50. Copyright 2015 Elsevier.

As it is known, the property of air stability is important for practical applications.^{54,55} The stability of device is influenced by the domain size and boundaries in the organic thin films. The air stability of devices fabricated with the WEG method has been demonstrated.⁵⁰ The FETs based on the highly ordered CuPc/*p*-6P thin film with large sizes of domains exhibit a better stability for 20 days in the ambient conditions. The devices based on the CuPc thin film with randomly aligned crystallites show a positive shifted threshold voltage, much lower I_{on}/I_{off} and mobility after being exposed to the ambient with the same temperature and humidity for 20 days. X-ray photoelectron spectroscopy (XPS) was performed to confirm the compositional changes in these films (Fig. 12). From XPS, it is proved that, as stored in the same conditions, the oxygen content in highly ordered CuPc/*p*-6P thin films with large-size domain is much less than that in CuPc thin films. Randomly aligned CuPc thin films have higher degree of misorientation and more boundaries, therefore much more oxygen and water diffused into the thin film with small-size crystallites to restrict the transport of charges and decrease the device stability. The film morphology is rationally optimized by the WEG method for high performance and air stable devices, which effectively reduces the physical absorption of the oxygen and water.

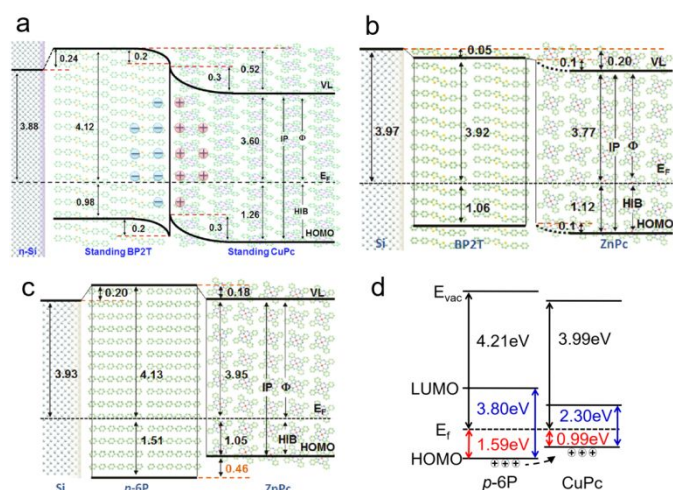


Fig. 13 UPS measured energy levels diagram of various heterojunctions.^{45,46,56} Reproduced with permission from ref. 45. Copyright 2016 WILEY-VCH Verlag GmbH & Co. KGaA, Weinheim. Reproduced with permission from ref. 46. Copyright AIP Publishing. Reproduced with permission from ref. 56. Copyright 2011, American Chemical Society.

The interfaces are intensively studied for a better performance in multi-layer devices, and the organic interfaces

possess amazing electronic properties, which are useful for the charge transfer in the optoelectronic devices. The fundamental mechanism of vertical charge transport in these high-quality thin films fabricated with WEG method has been elucidated. In order to determine the molecular orbital energy level of the organic heterojunctions, the measurements of ultraviolet photoelectron spectroscopy (UPS) were applied to detect the kinetic energy spectra of photoelectrons emitted from the molecules after absorbing ultraviolet photons. The UPS measured energy levels diagram of various heterojunctions prepared with WEG method are shown in Fig. 13.^{45,46,56} When two organic semiconductors are brought into contact, the junction is not yet in a steady state and a process is needed to get to thermal equilibrium. The charge redistribution occurred at the interface. As the electrons accumulate near the interface of the heterojunction, it is pictured as a downward band bending. With the band bending, thermal equilibrium is achieved after the movement of charge carriers. The UPS results of CuPc/BP2T thin film show the characteristics of the interface: in the CuPc layer, the upward band bending occurs, while in the BP2T layer, the downward bending of energy level occurs.⁴⁶ The holes accumulate in the CuPc layer and electrons accumulate in the BP2T layer. A conduction channel is thus formed at the interface of CuPc/BP2T. The conductivity of the device based on the CuPc/BP2T heterojunction thin film with an Ohmic behaviour is 3 orders of magnitude higher than that of the CuPc device. The conductivity is proportional to the mobility and concentration of charge carriers. In the UPS measurements, the gradual energy shift within 10 nm of the CuPc/BP2T heterojunction was observed, which is better to be described by a static band bending model. For BP2T, the energy level bending is about 0.2 eV and the ionization potential (IP) is 5.1 eV. For CuPc, the energy level bending is about 0.3 eV and the IP is 4.9 eV. Compared with the organic molecules with a lying-down configuration, the standing-up molecular assemblies have a little different energy level. The characteristics of charge transport could be tuned by changing the template layer with different energy levels.⁵⁶ In the FET based on the ZnPc/*p*-6P thin film prepared with the WEG method, the template layer of *p*-6P blocked the holes from the ZnPc layer. For ZnPc/BP2T devices, the template layer enables hole transport across the interface.

The morphology and interfacial interaction influence the accumulation of charge carriers and the interfacial electronic properties can be utilized to design functional devices. From UPS,⁴⁵ the work function (WF) and the highest occupied molecular orbital (HOMO) of CuPc layer grown on the template layer is smaller than the WF and HOMO of *p*-6P thin film, as shown in the deduced energy diagram in Fig. 13d. Holes move to higher energy levels and electrons vice versa. The potential between the two layers facilitates holes in *p*-6P layer to be transferred to the CuPc layer. In the photodetector based on highly ordered CuPc/*p*-6P thin film, the photo-generated holes in the *p*-6P layer are predicted to move to the CuPc layer under the electric field of the gate voltage. The heterojunction structure significantly reduces the recombination rate. Compared with the single-layer CuPc devices, by inserting a *p*-6P layer, the light absorption is enhanced and the CuPc/*p*-6P heterojunction improves the optoelectronic performance.

The heterojunction effect in the CuPc/*p*-6P thin films fabricated with the WEG method has also been studied with KPFM.⁵⁷ The corresponding surface electrical potential distribution of CuPc/*p*-6P and CuPc thin films has been directly mapped. The results indicate that, compared to the conventional polycrystalline films, the hole accumulation and band bending in the ordered CuPc/*p*-6P thin film are more obvious, which contributes to the crystal-like charge transport. Therefore, both the high mobility and heterojunction effect can be obtained in the highly ordered organic thin films.

4 Optoelectronic applications

4.1 Organic phototransistors

It is inefficient to dissociate excitons into mobile charges in the bulk of organic films with the same molecules. At the interface, the exciton dissociation in an organic heterojunction is much more efficient due to charge transfer across at the heterojunction.^{58,59} As discussed above, by using the method of WEG, the crystal domains coalesce to form a highly ordered organic thin film with larger domain sizes and less domain boundaries. The π - π stacking molecules with a standing-up arrangement improve the transport of charge carriers and the overall device performance. In these high-quality thin films fabricated with the WEG method, the template layer forms a heterojunction with the top layer. The heterostructure with specifically tailored spectroscopic properties further improves the performance under illumination. Light can be used as a wireless signal carrier, and can also be used to control biological cells with light-sensitive proteins in living tissues of nematodes, fruit flies, mice, and so on.⁶⁰⁻⁶² In organic optoelectronic devices, the organic heterojunctions absorb and convert the incident light into electrical current. Because the photogenerated charges need to travel through the organic layers, high mobility is also desirable for optoelectronic device with productive photoelectric conversion efficiency. Highly ordered organic heterojunction thin films prepared with the WEG method have been intensively studied and applied in photodetector, photomemory, photovoltaic cells, artificial optoelectronic synapse, and so on.^{28,45,63,64}

highly ordered CuPc/*p*-6P thin film prepared by WEG. The photoresponsivity at V_{on} as a function of (b) power intensity, (c) light source wavelength and (d) *p*-6P layer thickness.⁴⁵ Reproduced with permission from ref. 45. Copyright 2016 WILEY-VCH Verlag GmbH & Co. KGaA, Weinheim.

Photodetectors convert light information to electrical signals with amplification properties, which has application in health care and environmental monitoring. Phototransistor is a three-terminal optoelectronic device with a gate electrode. Light may also serve as an additional control terminal to generate photocarriers. Compared to two-terminal photodetectors, phototransistors have lower noise and higher sensitivity.¹⁹ The performance of organic phototransistors is dramatically affected by the morphology and grain size of the organic films. Noh *et al.* fabricated CuPc-single-layer phototransistors with a photoresponsivity of 2 A/W and photosensitivity of 3×10^3 , respectively.⁶⁵ Upon absorption of the incident photon, the photo-generated electron-hole pair must dissociate into constituent carriers. However, a single layer for the absorption of photon is not enough to achieve a high performance. The interface of a heterojunction can enhance the dissociation of excitons into mobile charges.^{66,67} Peng's group fabricated organic phototransistors based on a planar heterojunction of CuPc/PbPc.⁶⁸ The photosensitivity was 6.2×10^2 and photoresponsivity was just 77.4 mA/W. The high density of defects and boundaries restricted the carrier transport ability. Thus, a high-quality organic semiconductor thin film with high mobility is useful to improve the optoelectrical performance.

High-performance organic heterojunction phototransistors have been successfully fabricated with CuPc thin films grown on *p*-6P template layer with WEG.⁴⁵ Under 365nm UV light irradiation, the photoresponsivity and the ratio of photocurrent and dark current in CuPc/*p*-6P heterojunction phototransistors reached 4.3×10^2 A/W and 2.2×10^4 , respectively, which are much better than those in CuPc or *p*-6P phototransistors (Fig.14). In the CuPc/*p*-6P phototransistors, the bottom *p*-6P layer acted as the molecular template layer inducing the growth of highly ordered CuPc thin film. The charge transport was dramatically improved with less boundaries. Furthermore, the bottom *p*-6P layer formed the effective heterojunction with CuPc layer. The light absorption and dissociation of exciton was greatly enhanced. The optoelectrical performance is dependent on the wavelength of the light source, and the best performance is obtained in the device with a highly ordered thin film of thickness of 30 nm CuPc and 7.5 nm *p*-6P.

By effectively controlling the gate voltage and the external light terminal, multi-level storage can be realized in organic photomemory device that is based on phototransistor. Photomemory devices convert and store the incident optical signals into electrical signals and may serve as a building block for optical signal processing and photonic neuromorphic circuits. Benefiting from the heterojunction of organic channel layer and template layer, photomemory devices with VOPc (Vanadyl-Phthalocyanine)/*p*-6P heterojunction fabricated by WEG demonstrate direct converting to nonvolatile photocurrent for light information storage.⁶³ The light absorption and electron trapping capability are enhanced due to the effective VOPc/*p*-6P heterojunction. More importantly, after applying a light pulse,

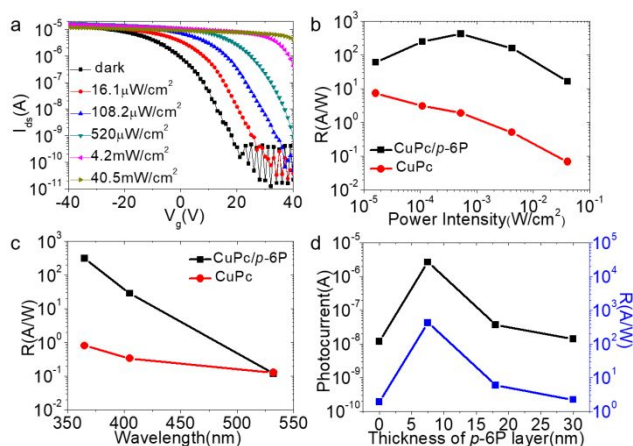


Fig. 14 (a) The typical transfer characteristics measured in the dark or under UV light with various light intensities of organic phototransistor based on

the light information is transformed to a photocurrent with a long relaxation time. 80% of photocurrent is sustained for about 5000 s. Multi-level storage by manipulating the pulse duration and light power intensity has also been achieved. The superior photomemory characteristics are mainly originated from efficient charge trapping at the interface.

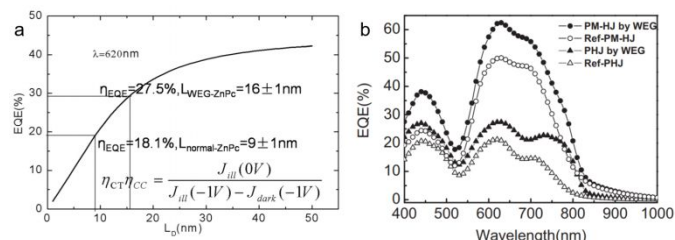


Fig. 15 (a) Calculated EQE for cell based on highly ordered ZnPc film by WEG as a function of ZnPc exciton diffusion length.⁶⁴ (b) EQE for organic photovoltaic cell based on planar heterojunction (PHJ) and planar-mixed heterojunction (PM-HJ) by WEG.⁶⁹ Reproduced with permission from ref. 64. Copyright AIP Publishing. Reproduced with permission from ref. 69. Copyright 2010 WILEY-VCH Verlag GmbH & Co. KGaA, Weinheim.

4.2 Organic photovoltaic cells

Organic photovoltaic cells (OPVs) are unique organic optoelectronic devices to convert solar energy into electrical energy. However, in many organic semiconductors, the exciton diffusion length is shorter than the optical absorption length, which limits the power-conversion efficiency (PCE). For example, in ZnPc film, the charge transport is controlled by the deep trap-filled process, and exciton diffusion length is around 9 nm (Fig. 15a). Because of the charge transport improvement from the shallow-trap-filling process and a low deep trap density, the exciton diffusion length is dramatic increased to 16 nm in the ZnPc film grown with WEG.⁶⁴ Thus, the highly ordered thin films with larger exciton diffusion length and superior charge transport are suitable for photovoltaic cells.

Based on a ZnPc/BP2T thin film prepared with the WEG method, a PCE of 3.07% was achieved in a ZnPc/C60 organic photovoltaic cell with a planar-mixed heterojunction (PM-HJ).⁶⁹ In the optoelectronic device, the BP2T layer acts as the template layer as well as the electron-blocking layer. The highly ordered ZnPc layer was deposited on the BP2T layer and plays the role of donor layer. The photo-response in the PM-HJ device prepared with WEG is much improved from 400 to 800 nm (Fig. 15b). The high-quality heterojunction thin film with few bulk traps improves the transport efficiency of free carriers dissociated from excitons at the interface, and reduces carrier recombination, which in turn enhance the short-circuit current and the filling factor. Furthermore, the PCE of OPV cells based on a vertically ordered bulk heterojunction film grown with WEG is also over 3%.⁷⁰ The size and distribution of C₆₀ crystalline grains on the ordered ZnPc thin film can also be controlled by varying the substrate temperature. The high performance was attributed to the phase separation in the vertical direction and more efficient carrier extract by an ordered structure.

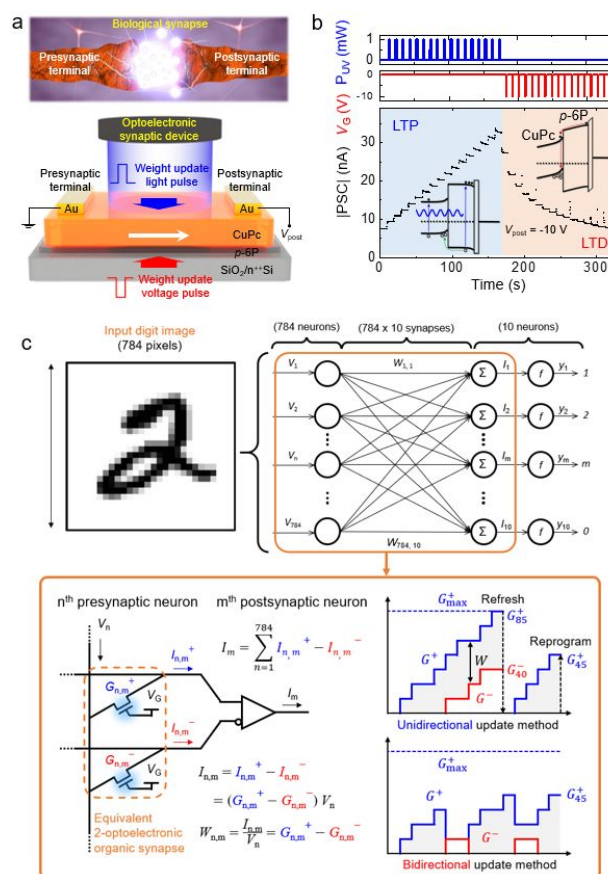


Fig. 16 (a) Schematic of a biological synaptic device containing light-sensitive protein and artificial optoelectronic synapse based on CuPc/p-6P thin film prepared by WEG modulated by optical and electrical pulses. (b) PSC responses under the application of continuous light pulses and voltage pulses. (c) Schematic illustration of single-layer-perceptron-based ANN and detailed weight updating processes based on unidirectional and bidirectional update methods.²⁸ Reproduced with permission from ref. 28. Copyright 2019 Elsevier Ltd.

4.3 Artificial synaptic devices

In order to stimulate the biological neural networks for complex recognition and neuromorphic computing, artificial optoelectronic synapse with processing and memory functions have been fabricated based on organic CuPc/p-6P heterojunction photomemory prepared by WEG method (Fig. 16).²⁸ In a biological synapse, synaptic weight between presynaptic and postsynaptic neurons is timely modulated by signal transmission from external stimuli. The artificial optoelectronic synapses implement optical-sensing and synaptic functions together, in which light acts as the input signal. Many biological synaptic functions, such as excitatory postsynaptic current (PSC)/inhibitory PSC, short-term plasticity, long-term potentiation (LTP), long-term depression (LTD), and artificial sensory functions, have been successfully mimicked by using light and voltage pulses for potentiating and depressing the synaptic weight, respectively. The feasibility for artificial neural network (ANN) in terms of the training/recognition tasks of the Modified National Institute of Standards and Technology (MNIST) digit image patterns has been confirmed on the artificial optoelectronic synapse based on a CuPc/p-6P thin film prepared with WEG. Under continuous light pulses, the stable and linearly

potentiated conductance states enhance the recognition rates to 78% for the MNIST digit patterns with the assistance of a unidirectional update method, even though the ANN is based on a single-layer perceptron model. The numbers of photogenerated holes supplied to the CuPc channel and photogenerated electrons trapped at the *p*-6P/dielectric interface is constant at every light pulse, resulting in this perfectly linear LTP characteristic.

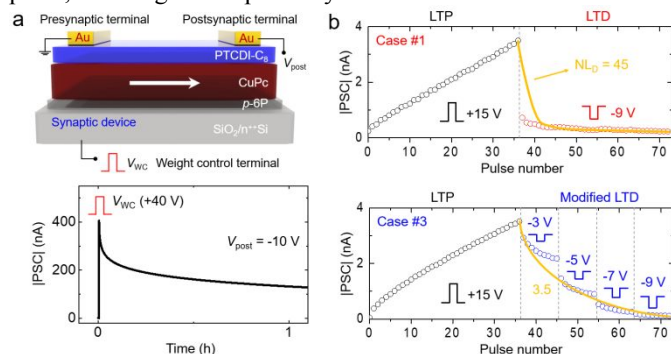


Fig. 17 (a) Schematic of artificial synaptic device based on PTCDI-C₈/CuPc/*p*-6P organic double-heterojunction structure and PSC response after application of single pulse. (b) LTP/LTD (modified LTD) characteristics under application of consecutive pulses.⁷¹ Reproduced with permission from ref. 71. Copyright 2020, American Chemical Society.

Artificial synaptic devices with non-volatile step modulation of the conductance triggered by the pulse of gate voltage have been successfully achieved (Fig. 17) based on a double heterojunction structure of *N,N'*-dioctyl-3,4,9,10-perylene tetracarboxylic diimide (PTCDI-C₈)/CuPc/*p*-6P.⁷¹ The highly ordered CuPc/*p*-6P thin film is also fabricated with the WEG method. The top PTCDI-C₈ layer acts as a hole-blocking layer to improve the long-term synaptic performance. The pulse-induced charge carriers are effectively confined in the CuPc layer sandwiched between the other two layers. Due to the novel device configuration designed by energy band engineering, the critical synaptic characteristics are successfully emulated. The linearity in the LTD region is improved a lot by a pulse modulation technique involving sequential application of voltage pulses. Furthermore, by application of the four-amplitude weight update method, the recognition rate of an ANN for MNIST digit images is enhanced considerably from 53% to 70%.

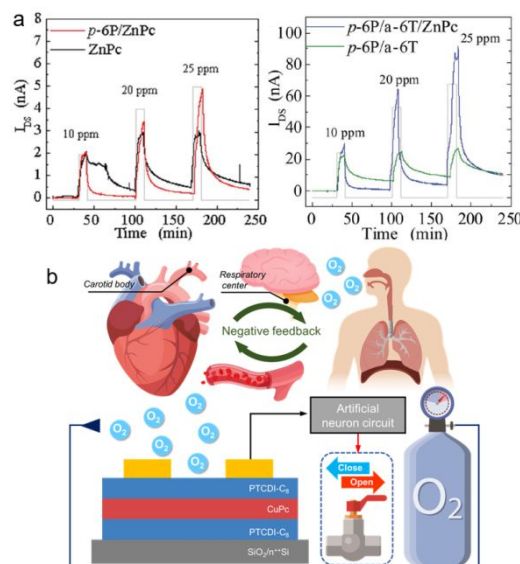


Fig. 18 (a) Dynamic response current of NO₂ sensors with different heterostructure as active layers.⁷² (b) Schematic illustration of negative feedback process for maintaining oxygen homeostasis in human body and artificial autonomic nervous system based on oxygen-sensitive trilayered organic double heterojunction.⁷³ Reproduced with permission from ref. 72. Copyright 2019 WILEY-VCH Verlag GmbH & Co. KGaA, Weinheim. Reproduced with permission from ref. 73. Copyright 2020 WILEY-VCH Verlag GmbH & Co. KGaA, Weinheim.

4.4 Organic gas sensors

Organic heterojunction can be used as smart gas sensor to open up new possibilities for the development of a biomimetic neural system that can respond appropriately to various environmental changes. The high performance NO₂ gas sensor has been fabricated based on the organic heterojunction ultrathin film prepared by the WEG method.^{72,74} The sensor with heterostructure of ZnPc/*p*-6P as active layer show higher dynamic current than the ZnPc-single-layer sensor (Fig. 18a).⁷² The properties of *p*-6P/ α -sexithiophene (α -6T)/ZnPc sensor is more remarkably enhanced than the sensor based on other structures, attributed to the easy gas adsorption of the morphology. When the active layer changed to the non-sensitive *N,N*-diphenyl perylene tetracarboxylic diimide (PTCDI-Ph), the gas sensor with accumulated heterojunction of PTCDI-Ph/*p*-6P also achieves a high sensitivity to NO₂ with quicker response and recovery at room temperature.⁷⁴ The highly ordered morphology improves the transport of charge carrier and enhances the signal produced. By depositing the VOPc layer on the top, the sensor with double-heterojunction of PTCDI-Ph/*p*-6P/VOPc achieves a significant increase in sensitivity. The relative response intensity is five times larger than that of the single-heterojunction sensor. In addition, an oxygen-sensitive artificial synaptic device based on the three-layered organic double heterojunction with the PTCDI-C₈/CuPc/PTCDI-C₈ structure was applied to the realization of a negative feedback system for regulation of oxygen homeostasis, which mimics the human autonomic nervous system (Fig. 18b).⁷³ The artificial synaptic transistors detect oxygen concentration and generates a synaptic signal simultaneously. The interconversion between the excitatory and inhibitory modes of the synaptic current at various oxygen concentrations is successfully achieved, due to the

oxygen-induced traps in the organic layer modulate the majority charge carrier from holes to electrons.

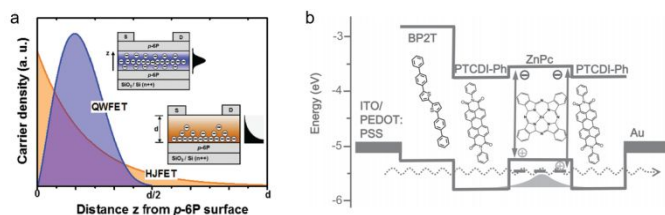


Fig. 19 (a) The carrier density in VOPc layer as a function of the distance away from bottom *p*-6P layer and carrier distribution in *p*-6P/VOPc/*p*-6P quantum well FET and VOPc/*p*-6P heterojunction FET.⁷⁵ (b) Energy diagram and molecular structures of an organic quantum well based on highly ordered crystalline heteroepitaxy BP2T/PTCDI-Ph/ZnPc/PTCDI-Ph film prepared by WEG.⁷⁶ Reproduced with permission from ref. 75. Copyright 2017 WILEY-VCH Verlag GmbH & Co. KGaA, Weinheim. Reproduced with permission from ref. 76. Copyright 2014 WILEY-VCH Verlag GmbH & Co. KGaA, Weinheim.

4.5 Quantum well OFET

Organic quantum well structure has been constructed on the basis of VOPc and *p*-6P sandwiched-heterostructure films, where VOPc acts as the well and *p*-6P acts as the barrier.⁷⁵ Based on the high-quality VOPc/*p*-6P heterojunction film prepared with WEG, a traditional OFET shows ambipolar transport with electron mobility of 2.3 cm²/Vs and hole mobility of 1.2 cm²/Vs, respectively. In the heterojunction OFET, when applied an appropriate gate voltage, corresponding charge carriers would be accumulated near the interface of VOPc and *p*-6P layer, and the maximum carrier density is at the surface of *p*-6P layer (Fig. 19a). With a voltage applied on the source and drain electrodes, charge carriers are injected into the channel and the channel current is established.

Compared with the traditional heterojunction OFET, the OFET based on the organic quantum wells shows a much higher electron mobility of over 10 cm²/Vs. This is because with the right gate voltage, electrons are accumulated, and transport channel forms in the interior of the VOPc layer. Free from interfacial scattering and traps, the quantum well OFET exhibits a highly efficient 2D electron transport. The formation of quantized energy levels and resonant tunnelling in another organic quantum wells of highly ordered crystalline heteroepitaxy BP2T/PTCDI-Ph/ZnPc/PTCDI-Ph films prepared with WEG have been demonstrated by optical absorption and a negative differential resistance effect.⁷⁶ These highly ordered crystalline thin films with smooth interfaces and more regular energy distribution fabricated with the WEG method provide the possibility for various functional organic devices.

5 Conclusions and outlook

This perspective presents the fabrication and applications of highly ordered MPC thin films grown on a template layer of *p*-6P or BP2T with the WEG method. With the substrate heating, the π - π interactions of molecules are stronger than the interactions between the molecules and the substrate. The

molecules stand up and the direction of π - π stacking is parallel to the substrate. The transport of charge carriers and the overall device performance has been greatly improved by the WEG method. The transport of charge carriers was detailed characterised by various characterization instruments. Furthermore, in these high-quality thin films, the template layer forms the effective heterojunction with the MPC layer. The heterostructure with specifically tailored spectroscopic properties further improved the performance under illumination.

However, there is much more can be done if the potential of highly ordered organic heterojunction thin films is to be fully realized. It is possible that the performance of optoelectronic devices could be further improved by using other compounds as template layer for MPC with optimal thickness. The micro devices in one highly ordered crystalline domain can be arranged in the preferred direction with the best charge conduction, and the property of anisotropic conductivity can be further studied. The potential applications of the organic quantum well devices prepared by WEG are yet to be fully explored. Much work is still ongoing on the transport of charge carriers and functional applications of highly ordered organic heterojunction thin films. Especially in the field of artificial synapses, the high performance organic heterostructure devices will likely be the one of importance in artificial optical nerves system for vision. The next step is to design the artificial intelligence robotic systems with artificial synaptic circuits and achieve that collected massive sensory data from the changes in the environment dynamically train the artificial neural network and affect the behaviours. The optimization and device engineering for the commercialization of functional applications are the goal.

Conflicts of interest

There are no conflicts to declare.

Acknowledgements

The work is supported in part by National Natural Science Foundation of China (61975241). Y. G. acknowledges the support by NSF DMR-1903962. C. Q. acknowledges the support from Hunan Normal University.

Notes and references

1. P. Peumans and S.R. Forrest, *Appl. Phys. Lett.*, 2001, **79**, 126.
2. M. Shtein, J. Mapel, J.B. Benziger and S.R. Forrest, *Appl. Phys. Lett.*, 2002, **81**, 268.
3. P. Peumans, S. Uchida and S.R. Forrest, *Nature*, 2003, **425**, 158.
4. J.H. Schön, C. Kloc, E. Bucher and B. Batlogg, *Nature*, 2003, **422**, 93.
5. S.W. Culligan, Y. Geng, S.H. Chen, K. Klubek, K.M. Vaeth and C.W. Tang, *Adv. Mater.*, 2003, **15**, 1176.
6. S.R. Forrest and M.E. Thompson, *Chem. Rev.*, 2007, **107**, 923.

7. H.F. Haneef, A.M. Zeidell and O.D. Jurchescu, *J. Mater. Chem. C*, 2020, **8**, 759.
8. Y. Yuan, G. Giri, A.L. Ayzner, A.P. Zoombelt, S.C.B. Mannsfeld, J. Chen, D. Nordlund, M.F. Toney, J. Huang and Z. Bao, *Nat. commun.*, 2014, **5**, 3005.
9. J. Takeya, M. Yamagishi, Y. Tominari, R. Hirahara, Y. Nakazawa, T. Nishikawa, T. Kawase, T. Shimoda and S. Ogawa, *Appl. Phys. Lett.*, 2007, **90**, 102120.
10. V. Kalihari, E.B. Tadmor, G. Haugstad and C.D. Frisbie, *Adv. Mater.*, 2008, **20**, 4033.
11. G. Horowitz, *Adv. Funct. Mater.*, 2003, **13**, 53.
12. M. Mladenović, N. Vukmirović and I. Stanković, *J. Phys. Chem. C*, 2013, **117**, 15741.
13. A.B. Chwang and C.D. Frisbie, *J. Appl. Phys.*, 2001, **90**, 1342.
14. R. Matsubara, N. Ohashi, M. Sakai, K. Kudo and M. Nakamura, *Appl. Phys. Lett.*, 2008, **92**, 242108.
15. G. Horowitz and M.E. Hajlaoui, *Synth. Met.*, 2001, **122**, 185.
16. A.K. Mahapatro, N. Sarkar and S. Ghosh, *Appl. Phys. Lett.*, 2006, **88**, 162110.
17. Dawen Li, Evert-Jan Borkent, Robert Nortrup, Hyunsik Moon, Howard Katz and Zhenan Bao, *Appl. Phys. Lett.*, 2005, **86**, 42105.
18. J. Yang, D. Yan and T.S. Jones, *Chem. Rev.*, 2015, **115**, 5570.
19. K.-J. Baeg, M. Binda, D. Natali, M. Caironi and Y.-Y. Noh, *Adv. Mater.*, 2013, **25**, 4267.
20. Y. Yuan and J. Huang, *Adv. Opt. Mater.*, 2016, **4**, 264.
21. H. Dong, H. Zhu, Q. Meng, X. Gong and W. Hu, *Chem. Soc. Rev.*, 2012, **41**, 1754.
22. W. Huang, B. Yang, J. Sun, B. Liu, J. Yang, Y. Zou, J. Xiong, C. Zhou and Y. Gao, *Org. Electron.*, 2014, **15**, 1050.
23. J. Xiong, B. Yang, J. Yuan, L. Fan, X. Hu, H. Xie, L. Lyu, R. Cui, Y. Zou, C. Zhou, D. Niu, Y. Gao and J. Yang, *Org. Electron.*, 2015, **17**, 253.
24. Y. Chen, W. Qiu, X. Wang, W. Liu, J. Wang, G. Dai, Y. Yuan, Y. Gao and J. Sun, *Nano Energy*, 2019, **62**, 393.
25. Y. Lee, J.Y. Oh, W. Xu, O. Kim, T.R. Kim, J. Kang, Y. Kim, D. Son, J.B.-H. Tok, M.J. Park, Z. Bao and T.-W. Lee, *Sci. adv.*, 2018, **4**, eaat7387.
26. S. Seo, S.-H. Jo, S. Kim, J. Shim, S. Oh, J.-H. Kim, K. Heo, J.-W. Choi, C. Choi, S. Oh, D. Kuzum, H.-S.P. Wong and J.-H. Park, *Nat. commun.*, 2018, **9**, 5106.
27. J. Sun, S. Oh, Y. Choi, S. Seo, M.J. Oh, M. Lee, W.B. Lee, P.J. Yoo, J.H. Cho and J.-H. Park, *Adv. Funct. Mater.*, 2018, **28**, 1804397.
28. C. Qian, S. Oh, Y. Choi, J.-H. Kim, J. Sun, H. Huang, J. Yang, Y. Gao, J.-H. Park and J.H. Cho, *Nano Energy*, 2019, **66**, 104095.
29. R.A. Nawrocki, R.M. Voyles and S.E. Shaheen, *IEEE Trans. Electron. Device*, 2016, **63**, 3819.
30. W. Zhang, R. Mazzarello, M. Wuttig and E. Ma, *Nat. Rev. Mater.*, 2019.
31. Z.D. Popovic, M.I. Khan, S.J. Atherton, A.-M. Hor and J.L. Goodman, *J. Phys. Chem. B*, 1998, **102**, 657.
32. T. Saito, W. Sisk, T. Kobayashi, S. Suzuki and T. Iwayanagi, *J. Phys. Chem.*, 1993, **97**, 8026.
33. A. Babajanyan, L. Enkhtur, B.-E. Khishigbadrakh, H. Melikyan, Y. Yoon, S. Kim, H. Lee, T. Kim, K. Lee and B. Friedman, *Curr. Appl. Phys.*, 2011, **11**, 166.
34. Z. Bao, A.J. Lovinger and A. Dodabalapur, *Appl. Phys. Lett.*, 1996, **69**, 3066.
35. Z. Bao, A.J. Lovinger and A. Dodabalapur, *Adv. Mater.*, 1997, **9**, 42.
36. J. Wang, H. Wang, X. Yan, H. Huang and D. Yan, *Appl. Phys. Lett.*, 2005, **87**, 93507.
37. M. Cinchetti, K. Heimer, J.-P. Wüstenberg, O. Andreyev, M. Bauer, S. Lach, C. Ziegler, Y. Gao and M. Aeschlimann, *Nat. Mater.*, 2009, **8**, 115.
38. L. Zhang, Y. Yang, H. Huang, L. Lyu, H. Zhang, N. Cao, H. Xie, X. Gao, D. Niu and Y. Gao, *J. Phys. Chem. C*, 2015, **119**, 4217.
39. J.H. Schon, S. Berg, C. Kloc and B. Batlogg, *Science*, 2000, **287**, 1022.
40. V.C. Sundar, J. Zaumseil, V. Podzorov, E. Menard, R.L. Willett, T. Someya, M.E. Gershenson and J.A. Rogers, *Science*, 2004, **303**, 1644.
41. C. Wang, H. Dong, W. Hu, Y. Liu and D. Zhu, *Chem. Rev.*, 2012, **112**, 2208.
42. M. Mas-Torrent and C. Rovira, *Chem. Rev.*, 2011, **111**, 4833.
43. S. Liu, W.M. Wang, A.L. Briseno, S.C.B. Mannsfeld and Z. Bao, *Adv. Mater.*, 2009, **21**, 1217.
44. J. Yang and D. Yan, *Chem. Soc. Rev.*, 2009, **38**, 2634.
45. C. Qian, J. Sun, L.-A. Kong, G. Gou, M. Zhu, Y. Yuan, H. Huang, Y. Gao and J. Yang, *Adv. Funct. Mater.*, 2017, **27**, 1604933.
46. F. Zhu, M. Grobosch, U. Treske, M. Knupfer, L. Huang, S. Ji and D. Yan, *Appl. Phys. Lett.*, 2011, **98**, 203303.
47. H. Wang, F. Zhu, J. Yang, Y. Geng and D. Yan, *Adv. Mater.*, 2007, **19**, 2168.
48. W. Gu, Y. Hu, Z. Zhu, N. Liu, J. Zhang and J. Wang, *Solid-State Electron.*, 2013, **89**, 101.
49. C. Qian, J. Sun, L. Zhang, H. Huang, J. Yang and Y. Gao, *J. Phys. Chem. C*, 2015, **119**, 14965.
50. C. Qian, J. Sun, L. Zhang, H. Xie, H. Huang, J. Yang and Y. Gao, *Synth. Met.*, 2015, **210**, 336.
51. L. Huang, C. Liu, B. Yu, J. Zhang, Y. Geng and D. Yan, *J. Phys. Chem. B*, 2010, **114**, 4821.
52. J.L. Brédas, J.P. Calbert, da Silva Filho, D. A. and J. Cornil, *Proceedings of the National Academy of Sciences*, 2002, **99**, 5804.
53. J.-L. Brédas, D. Beljonne, V. Coropceanu and J. Cornil, *Chem. Rev.*, 2004, **104**, 4971.
54. L. Li, Q. Tang, H. Li and W. Hu, *J. Phys. Chem. B*, 2008, **112**, 10405.
55. C. Reese and Z. Bao, *J. Mater. Chem.*, 2006, **16**, 329.
56. F. Zhu, M. Grobosch, U. Treske, L. Huang, W. Chen, J. Yang, D. Yan and M. Knupfer, *ACS Appl. Mater. Interfaces*, 2011, **3**, 2195.
57. H. Hai-Chao, W. Hai-Bo and Y. Dong-Hang, *Chinese Phys. Lett.*, 2010, **27**, 86801.

58. P. Peumans and S.R. Forrest, *Chem. Phys. Lett.*, 2004, **398**, 27.
59. J.J.M. Halls, C.A. Walsh, N.C. Greenham, E.A. Marseglia, R.H. Friend, S.C. Moratti and A.B. Holmes, *Nature*, 1995, **376**, 498.
60. E. Pastrana, *Nat. Methods*, 2011, **8**, 24.
61. A.D. Douglass, S. Kraves, K. Deisseroth, A.F. Schier and F. Engert, *Curr. Biol.*, 2008, **18**, 1133.
62. D. Huber, L. Petreanu, N. Ghitani, S. Ranade, T. Hromádka, Z. Mainen and K. Svoboda, *Nature*, 2008, **451**, 61.
63. C. Qian, J. Sun, L.-A. Kong, Y. Fu, Y. Chen, J. Wang, S. Wang, H. Xie, H. Huang, J. Yang and Y. Gao, *ACS Photonics*, 2017, **4**, 2573.
64. J. Yang, F. Zhu, B. Yu, H. Wang and D. Yan, *Appl. Phys. Lett.*, 2012, **100**, 103305.
65. Y.-Y. Noh, D.-Y. Kim and K. Yase, *J. Appl. Phys.*, 2005, **98**, 74505.
66. P. Peumans, A. Yakimov and S.R. Forrest, *J. Appl. Phys.*, 2003, **93**, 3693.
67. P.F. van Hutten, V.V. Krasnikov and G. Hadziioannou, *Synth. Met.*, 2001, **122**, 83.
68. Y. Peng, W. Lv, B. Yao, G. Fan, D. Chen, P. Gao, M. Zhou and Y. Wang, *Org. Electron.*, 2013, **14**, 1045.
69. B. Yu, L. Huang, H. Wang and D. Yan, *Adv. Mater.*, 2010, **22**, 1017.
70. B. Yu, H. Wang and D. Yan, *Nanotechnology*, 2013, **24**, 484006.
71. C. Qian, S. Oh, Y. Choi, S. Seo, J. Sun, J.-H. Park and J.H. Cho, *ACS Appl. Mater. Interfaces*, 2020, **12**, 10737.
72. Y. Zhu, Q. Xie, Y. Sun, L. Wang, Q. Sun and L. Wang, *Adv. Mater. Interfaces*, 2020, **7**, 1901579.
73. C. Qian, Y. Choi, Y.J. Choi, S. Kim, Y.Y. Choi, D.G. Roe, M.S. Kang, J. Sun and J.H. Cho, *Adv. Mater.*, 2020, **32**, 2002653.
74. S. Ji, H. Wang, T. Wang and D. Yan, *Adv. Mater.*, 2013, **25**.
75. P. Zhang, H. Wang and D. Yan, *Adv. Mater.*, 2017, **29**, 1702427.
76. Z. Wang, T. Wang, H. Wang and D. Yan, *Adv. Mater.*, 2014, **26**.